ANALYSIS OF SUB-CM CHEMICAL ENDMEMBERS WITH THE MARS SCIENCE LABORATORY ALPHA PARTICLE X-RAY SPECTROMETER: A DEMONSTRATED IMPROVEMENT IN DERIVED ELEMENTAL STOICHIOMETRY. S. J. VanBommel<sup>1</sup>, J. A. Berger<sup>2</sup>, R. Gellert<sup>3</sup>, C. D. O'Connell-Cooper<sup>4</sup>, M. A. McCraig<sup>3</sup>, L. M. Thompson<sup>4</sup>, A. S. Yen<sup>5</sup>, J. R. Christian<sup>1</sup>, A. L. Knight<sup>1</sup>, and N. I. Boyd<sup>3</sup>; <sup>1</sup>Washington University in St. Louis, St. Louis, MO, USA; <sup>2</sup>Jacobs JETSII Contract, Houston, TX, USA; <sup>3</sup>University of Guelph, Guelph, ON, Canada; <sup>4</sup>University of New Brunswick, Fredericton, New Brunswick, Canada; <sup>5</sup>Caltech/NASA Jet Propulsion Laboratory, Pasadena, CA, USA.

**Introduction:** Since landing in Gale crater in August of 2012, the Mars Science Laboratory (MSL) rover *Curiosity* has climbed nearly 650 m in elevation by the end of 2022 and has acquired approximately 1,300 analyses with its in situ geochemical analysis instrument, the Alpha Particle X-ray Spectrometer (APXS) [1]. When deployed to its closest approach distance from a geologic target (18 mm separation between sample surface and instrument face), the analytical field of view (FOV) is 15 mm in diameter [2, 3].

Mars as a laboratory field site presents numerous challenges for in situ X-ray spectroscopy (e.g., [4]). With limited sample preparation and arm placement (accuracy) uncertainty typically on the scale of the diameter of the APXS FOV, heterogeneities within a target area, such as a ~5 mm calcium-sulfate vein cross-cutting bedrock, contribute an unknown fraction of the signal acquired by the instrument. The derivation of the composition of a single APXS spot assumes a homogeneous sample in order to determine and correct for matrix effects (e.g., the attenuation of induced X-rays by other elements within the sample). In the case of a calcium-sulfate vein within a typical Mars bedrock, the absorption of sulfur X-rays, for example, differs significantly when emitted from CaSO4·nH2O, as opposed to from within a silicate rock.

Previous work (e.g., [2, 3, 5, 6]) has derived the composition of chemically distinct visible endmembers through the use of APXS rasters. The deconvolution employed utilized APXS oxide data, data that were themselves calculated assuming a homogenous sample. Given the known presence of sub-cm-scale heterogeneities, these data in particular are susceptible to skewed matrix effects. In [7], the authors use the Sayunei 5-spot raster (sol 165) as a proof of concept for the new deconvolution approach given a the suitability of a Ca-S vein as a post-landing "calibration dataset". The same target was the catalyst for the entire raster deconvolution approach, first presented in [2], in order to answer the question: does a calcium-sulfate vein within APXS placement uncertainty explain all Ca- and S-enrichment within the observed data, or does the bedrock itself have a Ca-S-rich matrix? The work of [2] demonstrated that the former was true, localizing the raster within placement uncertainty that associated all excess Ca and S to the vein endmember, albeit with a molar S:Ca ratio of 1.3:1. This ratio deviates from the ideal 1:1 stoichiometry of CaSO<sub>4</sub>, but it was not an unexpected result, given the aforementioned homogeneity assumption and use of oxide data for input.

Here we present an improvement to this method through the utilization of lower-order data products, namely APXS spectra and spectral parameters. The results illustrate a significant improvement in the accuracy of derived endmember elemental ratios, the results of which ultimately advance *Curiosity*'s in situ mineralogical diagnostic capabilities.

**Method:** The work presented herein builds off of [2] and [3] through the input of APXS spectra and spectral parameters into a deconvolution algorithm which minimizes a non-invertible and bounded least-squares matrix equation to iteratively determine both the relative abundance (via FOV localization) and composition of a fixed number of endmembers. This is discussed in more detail by [7].

In addition to summarizing some results from [7], we revisit published APXS raster analyses presented in [2] and [3] to check whether any significant changes in the derived results have been observed, and, if so, what they inform. In all instances we utilized the relative endmember proportions derived within [2] and [3] and do not reinitiate APXS FOV localization. All input were corrected for atmospheric attenuation which primarily affects low-Z elements (i.e., Na, Mg).

**Results:** Analysis of the Sayunei vein using spectral parameters produced a S:Ca ratio of  $(0.96\pm0.21)$ :1 [7]. This demonstrates a significant improvement over the oxide method result of 1.3:1 [2] and provided confidence in the ultimate objective of [7]: to determine the chemical composition of mm-scale nodules. The nodular material was found to have  $(1.00\pm0.13)$ :1 S:Ca and  $(2.21\pm0.35)$ :1 P:Mn molar ratios, pointing to a likely 2:1 P:Mn phase associated with the Ca-sulfate.

The work of [3] looks into three additional raster targets we can apply the same approach to: the Mg-Ni-sulfate-rich nodule "Morrison" (sol 774), the Mn-sulfate-rich nodule "Sperrgebiet" (sol 1278), and the striking light and dark contrasting vein target Alvord Mountain (sol 937).

In the case of Morrison, the updated deconvolution derived compositional results within 3% (relative) for all major species, including the key elements of Mg, S, and Ni within the nodule (e.g., Fig. 1). The derived updated composition of Spergebiet offered less modest changes in major species, likely given the weaker chemical gradient, a consequence of only slight variability in endmember coverage. The improved result prompts a reduction of the molar Mg:S ratio from 1.5:1 to 1.3:1. This translates to an decreased Mg:S ratio, with the extra S possibly associated with newly inferred species P, Mn, Ni, and/or Zn (Fig. 1).

The Alvord Mountain raster perhaps contains the cleanest white (calcium sulfate) vein of significant areal extent interrogated with APXS thus far. Within the oxide deconvolution, the molar S:Ca ratio was around 1.10:1; under the improved method, the ratio achieved was 0.97:1. The dark vein endmember, noted for its Ca, Zn, and Ge enrichments [8], retained these noted enrichments in the updated analysis, but dropped all attribution of sulfur (~5 wt% SO<sub>3</sub> in the oxide method).

**Discussion:** The results discussed herein illustrate that the conclusions derived within the existing literature that utilized derived oxides for input remain valid. For endmembers of diverse composition, the former results are very similar to those newly derived. This is not unexpected given the mixed nature of these endmembers and the fact the homogeneity assumption holds more true. The application of this method to the Sperrgebeit nodule still suggests a different (or evolving) fluid within Gale when contrasting with the Morrison result, as noted previously by [3], even with the hint of the potential addition of P, Mn, Ni, and/or Zn within the chemical fingerprint of the earlier fluid(s).

Where the most significant differences were found were within endmembers whose composition significantly deviates from its surrounding. In the case of Morrison for example, there was ~11% Mg-Ni-sulfate added to the host bedrock to form the nodule [2]; not a major difference in composition. In contrast, the calcium sulfate veins have much higher purity than the Mg-sulfate nodules, thus the difference is more pronounced, and the application of the homogeneity assumption when the surrounding silicate bedrock is also in the FOV is stretched to the tune of significant deviations within molar ratios in the results derived from the oxide method. This is demonstrated by the near 1:1 S:Ca ratio with the new method in the white vein at both Sayunei and Alvord Mountain, a 10-30% improvement in accuracy.

Summary and Future Work: The interpretation of past results presented by [2], [3], [5], [6], and others using APXS oxide deconvolution method are unaltered. The derived composition of heterogeneous endmembers remains largely unchanged with the improved method, and where changes were observed the interpretation was unaffected. Mineralogical diagnoses benefit from spectral deconvolution, especially when the potential species are not immediately obvious (e.g., P-Mn enrichment within the Ayton and Groken workspace; sol 2857 [7, 9]). This capability will be particularly beneficial to constrain the distribution and types of sulfates within the sulfate unit that *Curiosity* is exploring on the flanks of Mount Sharp.

The ability to potentially resolve elemental ratios at a sub-FOV level and respectable accuracy with the APXS additionally provides an opportunity for analyses in concert with CheMin XRD mineralogy data. The mechanics noted here, combined with the spectral simulation capabilities of [10, 11], enable a reverse workflow whereby CheMin mineral abundances are converted into APXS spectral parameters. These parameters are compared to the acquired APXS data and used to better constrain amorphous content within the CheMin sample. Using this pipeline as a training set has the potential to enable in situ mineralogical inferences with APXS, absent CheMin analyses, through the implementation of machine learning techniques.

Acknowledgements: This work was supported by NASA MSL Participating Scientist Grant #80NSSC22K0650. A special thank-you to NASA/JPL for their support, dedication, and expertise during development and operations of the MSL mission as well as to colleagues past and present.

## **References:**

- [1] Gellert & Clark (2015), *Elements*, 11.
- [2] VanBommel et al. (2016), XRS, 45.
- [3] VanBommel et al. (2017), XRS, 46.
- [4] VanBommel et al. (2023), RSC, 11.
- [5] Stein et al. (2018), *JGR:P*, 123.
- [6] Arvidson et al. (2016), Am. Min, 101.
- [7] VanBommel et al. (2023), *Icarus*, 392.
- [8] Berger et al. (2017), JGR:P, 122.
- [9] Berger et al. (2021), *LPSC*, 2548.
- [10] VanBommel et al. (2019), *NIM:B*, 441.
- [11] VanBommel et al. (2019), Acta Ast., 165.

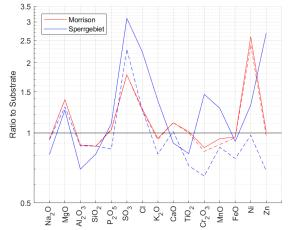


Figure 1: Nodule composition relative to substrate as derived from oxides (dashed) and spectral parameters (solid).